Ultrahigh-resolution optical coherence tomography with a diode-pumped broadband Cr^{3+}:LiCAF laser

Philipp C. Wagenblast, Tony H. Ko, James G. Fujimoto and Franz X. Kaertner

Department of Electrical Engineering and Computer Science and Research Laboratory of Electronics, Massachusetts Institute of Technology, Cambridge, MA 02139
pcw@mit.edu

Uwe Morgner

Max-Planck-Institut für Kernphysik, Heidelberg, Germany

Abstract: Ultrahigh resolution optical coherence tomography (OCT) is performed with a broadband, Kerr-lens mode-locked, diode-pumped Cr^{3+}:LiCAF laser. The laser source has a bandwidth of 89 nm with an output power of 37 mW. OCT imaging is demonstrated with 4.5 μm axial resolution in air or 3.4 μm in tissue. In vivo imaging of the human retina is demonstrated. Ultrahigh resolution OCT images from the Cr^{3+}:LiCAF laser source were compared with standard resolution images from a commercial OCT system and ultrahigh resolution OCT images from a Kerr-lens mode-locked Ti:sapphire laser light source. The Cr^{3+}:LiCAF source is pumped only by two single-emitter laser diodes, which makes this laser a viable, low-cost alternative to mode-locked Ti:sapphire lasers that are currently used for ultrahigh resolution OCT imaging.

OCIS codes: (170.4500) optical coherence tomography; (170.3880) medical and biological imaging; (140.4050) mode-locked lasers; (320.7090) ultrafast lasers

References and links:

1. D. Huang, E. A. Swanson, C. P. Lin, J. S. Schuman, W. G. Stinson, W. Chang, M. R. Hee, T. Flotte, K.Gregory, C. A. Puliafito, J. G. Fujimoto, "Optical coherence tomography," Science **254**, 1178-1181 (1991).
2. A. F. Fercher, W. Drexler, C. K. Hitzenberger, T. Lasser, "Optical coherence tomography - principles and applications," Rep. Prog. Phys. **66**, 239-303 (2003).
3. T. H. Ko, D. C. Adler, J. G. Fujimoto, D. Mamedov, V. Prokhorov, V. Shidlovski, S. Yakubovich, "Ultrahigh resolution optical coherence tomography imaging with a broadband superluminescent diode light source," Opt. Express **12**, 2112-2119 (2004), http://www.opticsexpress.org/abstract.cfm?URI=OPEX-12-10-2112
4. B. Bouma, G. J. Tearney, S. A. Boppart, M. R. Hee, M. E. Brezinski, J. G. Fujimoto, "High-resolution optical coherence tomographic imaging using a mode-locked Ti:Al_2O_3 laser source," Opt. Lett. **20**, 1486-1488 (1995).
5. W. Drexler, U. Morgner, F. X. Kaertner, C. Pitris, S. A. Boppart, X. D. Li, E. P. Ippen, J. G. Fujimoto, "In vivo high resolution optical coherence tomography," Opt. Lett. **24**, 1221-1223 (1999).
6. W. Drexler, U. Morgner, R. K. Ghanta, F. X. Kaertner, J. S. Schuman, J. G. Fujimoto, "Ultrahigh resolution ophthalmic optical coherence tomography," Nature Med. **7**, 502-50789 (2001).
7. A. Unterhuber, B. Povazay, B. Hermann, H. Sattmann, W. Drexler, V. Yakovlev, G. Tempea, C. Schubert, E. M. Anger, P. K. Ahnelt, M. Stur, J. E. Morgan, A. Cowey, G. Jung, T. Le, A. Stingl, "Compact low-cost Ti.Al_2O_3 laser for in vivo ultrahigh resolution optical coherence tomography," Opt. Lett. **28**, 905-907 (2003).
8. D. L. Marks, A. L. Oldenburg, J. J. Reynolds, S. A. Boppart, "Study of an ultrahigh-numerical-aperture fiber continuum generation source for optical coherence tomography," Opt. Lett. **27**, 2010-2012 (2002).
9. I. Hartl, X. D. Li, C. Chuboda, R. K. Ghanta, T. H. Ko, J. G. Fujimoto, "Ultrahigh-resolution optical coherence tomography using continuum generation in an air-silica microstructure optical fiber," Opt. Lett. **26**, 608-610 (2001).
10. B. Povazay, K. Bizheva, A. Unterhuber, B. Hermann, H. Sattmann, A. F. Fercher, W. Drexler, A. Apolonski, W. J. Wadsworth, J. C. Knight, P. St. J. Russel, M. Vetterlein, E. Scherzer, "Submicrometer axial resolution optical coherence tomography," Opt. Lett. **27**, 1800-1802 (2002).
11. Y. Wang, Y. Zhao, J. S. Nelson, Z. Chen, R. Windeler, "Ultrahigh-resolution optical coherence tomography by broadband continuum generation from a photonic crystal fiber," Opt. Lett. **28**, 182-184 (2003).

#4498 - $15.00 US Received 1 June 2004; revised 7 July 2004; accepted 7 July 2004

12. S. Bourquin, A. D. Aguirre, I. Hartl, P. Hsiung, T. H. Ko, J. G. Fujimoto, T. A. Birks, W. J. Wadsworth, U. Buenting, D. Kopf, "Ultrahigh resolution realtime OCT imaging using a compact femtosecond Nd :Glass laser and nonlinear fiber," Opt. Expr. **11**, 3290-3297 (2003), http://www.opticsexpress.org/abstract.cfm?URI=OPEX-11-24-3290
13. P. Wagenblast, R. Ell, U. Morgner, F. Grawert, F. X. Kaertner, "10-fs, diode-pumped Cr^{3+}:LiCAF laser," Opt. Lett. **28**, 1713-1715 (2003).
14. S. Uemura, K. Torizuka, "Development of a Diode-Pumped Kerr-Lens Mode-Locked Cr:LiSAF laser," IEEE J. Quant. El., **39**, 68-73 (2003).
15. J. Herrmann, "Theory of Kerr-lens mode-locking: role of self-focusing and radially varying gain," J. Opt. Soc. Am. **B 11**, 498-512 (1994).
16. F. X. Kaertner, N. Matuschek, T. Schibli, U. Keller, H. A. Haus, C. Heine, R. Morf, V. Scheuer, M. Tilsch, T. Tschudi, "Design and fabrication of double-chirped mirrors," Opt. Lett. **22**, 831-833 (1997).
17. E. A. Swanson, J. A. Izatt, M. R. Hee, D. Huang, C. P. Lin, J. S. Schuman, C. A. Puliafito, J. G. Fujimoto, "In vivo retinal imaging by optical coherence tomography," Opt. Lett. **18**, 1864-1866 (1993).
18. M. R. Hee, J. A. Izatt, E. A. Swanson, "Optical coherence tomography of the human retina," Archives of Ophthalmology **113**, 325-332 (1995).
19. M. R. Hee, C. A. Puliafito, J. S. Duker, "Topography of diabetic macular edema with optical coherence tomography," Ophthalmology **105**, 360-370 (1998).
20. A. M. Kowalevicz, T. R. Schibli, F. X: Kaertner, J. G. Fujimoto, "Ultralow threshold Kerr-lens mode-locked Ti:Al_2O_3 laser," Opt. Lett. **27**, 2037-2039 (2002).

1. Introduction

Optical coherence tomography (OCT) is an emerging technique for high-resolution, two-dimensional *in vivo* biomedical imaging [1,2]. In OCT, the cross-correlation function of a temporally low-coherence source is used to measure axial scattering from the sample. By scanning the beam across the tissue, a two-dimensional cross-sectional image of the internal tissue structure can be obtained. The coherence length of the light source gives the axial resolution, which is inversely proportional to the bandwidth. Commercial ophthalmic OCT systems use superluminescent diodes (SLD) as low-coherence light source. SLDs typically have 20-30 nm bandwidth and give an axial resolution of 10-15 µm. Broader bandwidth superluminescent diode light sources have recently been used for ultrahigh-resolution OCT imaging [3], but they currently have limited output power of a few mW, which is insufficient for many imaging applications. In order to increase the axial resolution of OCT imaging, broadband mode-locked lasers have been used. Both broadband light directly from a laser [4-7] and laser light externally broadened in either high numerical aperture optical fiber [8] or microstructured fiber [9-11] have been utilized to demonstrate outstanding axial resolution of 1-2 µm. Lasers that are directly diode-pumped are promising candidates for widespread use because of the reduced cost and complexity of the pump laser as compared to the frequency-doubled pump sources required in Ti:sapphire systems. This approach has been applied with a diode-pumped Nd:glass femtosecond laser in combination with external broadening in a nonlinear fiber to yield OCT resolution of 4 µm [12].

The approach in this study is to use the diode-pumped femtosecond laser directly as the light source for ultrahigh-resolution OCT imaging. We have recently developed a 10-fs Kerr-lens mode-locked Cr^{3+}:LiCAF laser [13], which generates broad spectra with bandwidth exceeding 150 nm, and has sufficiently high output power to serve as a source for ultrahigh resolution OCT. However, the spectrum of this laser exhibits relatively strong modulation due to non-uniformity in dispersion compensation. For OCT applications, a smooth spectral shape is indispensable because the structured spectrum would generate satellites in the interferometric point spread function (PSF) of the system. Pedestals and satellites originating from spectral features should be reduced because they degrade image contrast and produce artifacts. In order to use a Kerr-lens mode-locked Cr^{3+}:LiCAF for OCT imaging, it is necessary to achieve a smooth, Gaussian-like output spectrum, while preserving as much bandwidth and output power as possible.

The diode-pumped Kerr-lens mode-locked Cr^{3+}:LiCAF laser has a bandwidth of 89 nm and an output power of 37 mW. Ultrahigh resolution OCT imaging is demonstrated with 4.5 µm axial resolution in air or 3.4 µm in tissue. In vivo imaging of the human retina is

#4498 - $15.00 US Received 1 June 2004; revised 7 July 2004; accepted 7 July 2004

performed and OCT images using the Cr^{3+}:LiCAF laser source are compared with standard resolution images from a commercial ophthalmic OCT system and ultrahigh resolution OCT images from a Kerr-lens mode-locked Ti:sapphire laser light source. The Cr^{3+}:LiCAF laser achieves much better resolution images than standard OCT systems and approaches the image resolutions achieved using Ti:sapphire lasers. The mode-locked Cr^{3+}:LiCAF laser has the advantage of being directly diode-pumped and is significantly lower cost and complexity than Ti:sapphire technology.

2. Cr^{3+}:LiCAF laser light source

Diode-pumped, mode-locked Colquiriite sources have been demonstrated to generate very broad spectra with bandwidth exceeding 150 nm and output powers on the order of tens of mW [13,14]. The Cr^{3+}:LiCAF laser used in this study is pumped by the orthogonally polarized beams from two broad-area laser diodes (Coherent S-670-500C) with 500 mW optical power, each in an elliptical multimode beam. The emitter size of the diodes are 1×100 µm. Along the fast diverging axis, the beam is close to diffraction limited, whereas it is multimode along the slow diverging axis with a beam propagation M^2 factor of 15 to 18. Along the fast axis direction, a cylindrical fiber-collimating lens reduces the beam divergence. The collimation results in an elliptical pump beam with an aspect ratio of slow to fast axis of about 4, where the ellipticity does not change as the beam is transformed by spherical optics. As a result of the collimation, the Rayleigh distances in both planes of the beam are equal, and they can be mode-matched simultaneously. The Cr^{3+}:LiCAF laser crystal is 2 mm long and has a nominal 10% doping concentration that results in an absorption length of 0.7 mm for the pump light. High doping increases the small signal gain in a diode-pumped LiCAF laser, where reabsorption does not affect the laser performance. The Rayleigh range of the pump beam is matched to half the absorption length by focusing the beam to a radius of 30×8 µm in the slow and fast axis, respectively. This is accomplished using a telescope consisting of achromatic doublet lenses of 100 mm and 50 mm focal lengths. The absorbed pump power is approximately 850 mW.

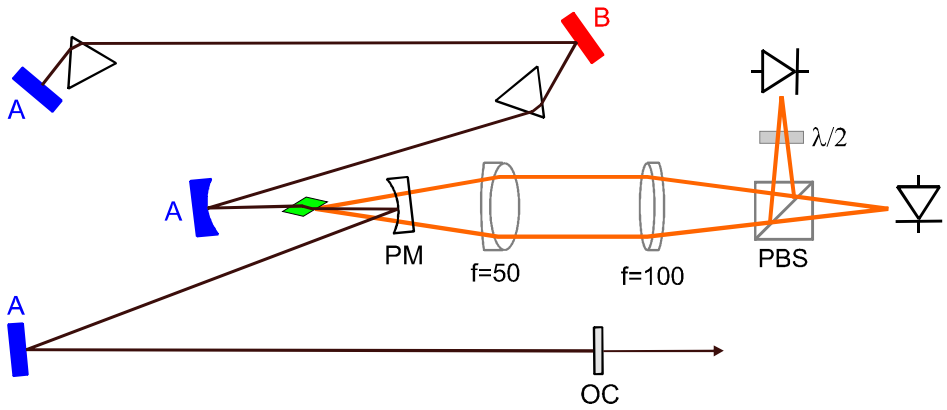

Fig. 1. Schematic of the laser setup. Blue and red mirrors A and B are DCM with dispersion characteristics of Fig. 2. PBS: polarizing beam splitter, OC: output coupler, PM: pump mirror, λ/2: half wave plate.

A schematic of the laser setup is shown in Fig. 1. The laser was made compact by increasing the repetition rate to 165 MHz and by folding the z-design cavity two more times than the previously reported layout [13]. The resonator eigenmode is focused into the laser crystal by two mirrors with 75 mm radius of curvature. Using this design, the laser size is 20×30 cm. The laser, the pump diodes and optics, and the fiber-coupling unit are integrated on a 30×60 cm optical board. In continuous wave operation, the laser emits up to 90 mW of power

#4498 - $15.00 US
Received 1 June 2004; revised 7 July 2004; accepted 7 July 2004

through a 0.8% output coupler. The short absorption length in the highly Cr-doped crystal results in a high inversion density leading to strong gain guiding, which enhances the effect of the Kerr lens and the fast saturable absorber action [15]. The strongest Kerr-lensing occurs for resonator settings that are beyond the stability limits of the unpumped resonator without gain guiding. In this way, it is possible to exploit pure soft-aperture Kerr-lens mode-locking in this diode-pumped laser, thus resulting in stable pulsed operation. The laser is not self-starting, but mode-locked operation can be started by mechanically perturbing one of the laser mirrors, such as the output coupler. This starting mechanism is similar to that used in Ti:sapphire lasers.

The dispersion compensation of the laser is carried out by a combination of double-chirped mirrors (DCMs) [16], generating sufficient negative second-order dispersion, and a fused silica prism sequence for adjusting the second- and third-order dispersion. Except for the pump mirror and the output coupler, which have low dispersion over the lasing bandwidth, all mirrors are dispersion-compensating DCMs. The prisms are essential for higher order dispersion compensation [13].

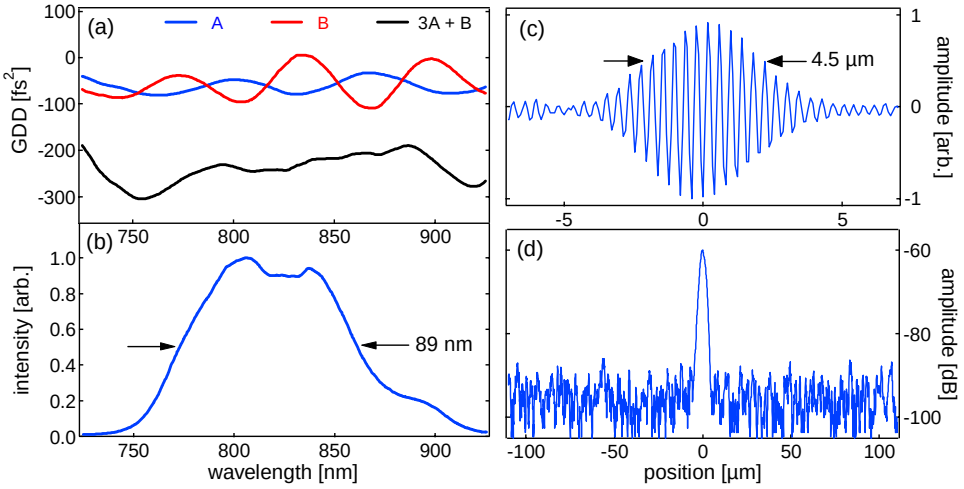

Fig. 2. (a) Dispersion characteristics of the double-chirped mirrors, and (b) mode-locked spectrum of the laser. (c) Interferometric point spread function of the imaging system in air. (d) Demodulated logarithmic point spread function of the OCT imaging system. The resolution is 4.5 µm in air, which corresponds to 3.4 µm in biological tissue.

The point spread function (PSF) of the OCT imaging system depends crucially on the spectrum of the light source used, which ideally should have a smooth Gaussian shape [2] rather than the strongly modulated spectrum from our previous LiCAF laser [13]. Since the spectral shape of the broadband Cr^{3+}:LiCAF laser is predominantly influenced by dispersion characteristics, we accomplish spectral shaping by using a combination of DCMs to achieve an overall smooth dispersion within one round-trip in the resonator and a significant reduction of spectral modulation. The dispersion of the mirrors as measured by white light interferometry is shown in Fig. 2(a). Mirror A has a dispersion oscillation magnitude of 45 fs^2, whereas oscillations of mirror B have a magnitude of 110 fs^2, with the oscillation out of phase with mirror A's oscillation. The dispersion of a combination of 3:1 reflections on the two different mirror sets is also shown in Fig. 2(a). Between 750 and 900 nm wavelengths, a near perfect cancellation of dispersion oscillations can be achieved. For practical reasons, 5:2 reflections on mirrors of type A and B are used instead of the optimum 6:2. This combination results in sufficiently flat dispersion characteristics so that broadband emission is obtained with a smooth mode-locked spectrum. The mode-locked spectrum in Fig. 2(b) is centered at

#4498 - $15.00 US
Received 1 June 2004; revised 7 July 2004; accepted 7 July 2004

815 nm and has a modulation-free, nearly Gaussian shape with a full-width half-maximum bandwidth of 89 nm. The output power of the mode-locked laser is 37 mW. The bandwidth is limited by higher order dispersion terms of the intracavity prisms. The Cr^{3+}:LiCAF gain bandwidth should enable the generation of an output bandwidth of well above 130 nm. With further optimized DCM designs, which have more accurate dispersion compensation, prismless operation with broader bandwidths should be achievable.

3. OCT imaging

In order to demonstrate imaging of the human retina, an ultrahigh resolution ophthalmic OCT system was used. A schematic of the OCT system is depicted in Fig. 3. The fiber-optic interferometer and other optical components of the OCT system are optimized to support the broad bandwidth of the laser light source in order to maintain ultrahigh resolution throughout the OCT system. Dispersion between the reference and sample arms of the interferometer is carefully balanced by using optical materials of identical thickness in both arms. A high-speed, high-sensitivity, low-noise electronic detection system was built in order to achieve OCT imaging with high dynamic range and high sensitivity. A computer controls the scanning pattern of the OCT beam on the retina, acquires data, and generates an OCT image on the display in real time. The imaging system in the sample arm is based on a slit lamp biomicroscope, which has an integrated CCD to provide a video image of the fundus of the eye. The subject's eye position is established by using internal fixation targets which are inside the slit lamp illuminator and visible to the subject in the same eye that is being imaged. After scanning was completed, the axial motion artifacts in the image can be corrected using standard cross-correlation algorithms [17].

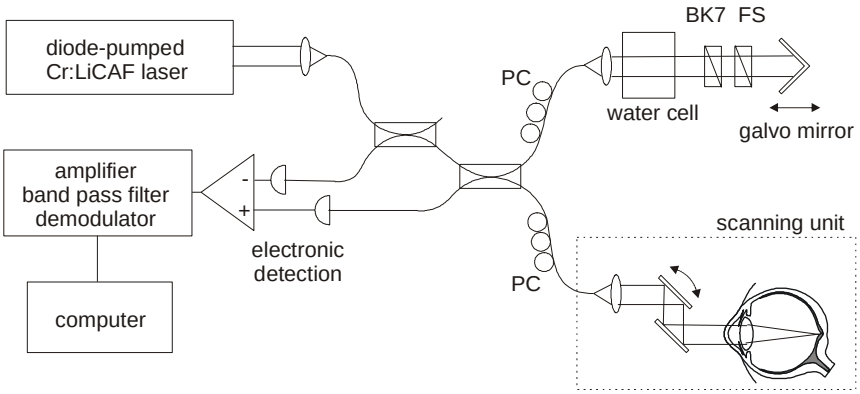

Fig. 3. Schematic of the fiber-optic ultrahigh resolution ophthalmic OCT imaging system. Dispersion compensation of the slit lamp optics is achieved by using BK7 and fused silica (FS) prisms while the water cell compensates the dispersion from the vitreous body of the eye. The polarization is adjusted separately by the controllers (PC).

#4498 - $15.00 US Received 1 June 2004; revised 7 July 2004; accepted 7 July 2004

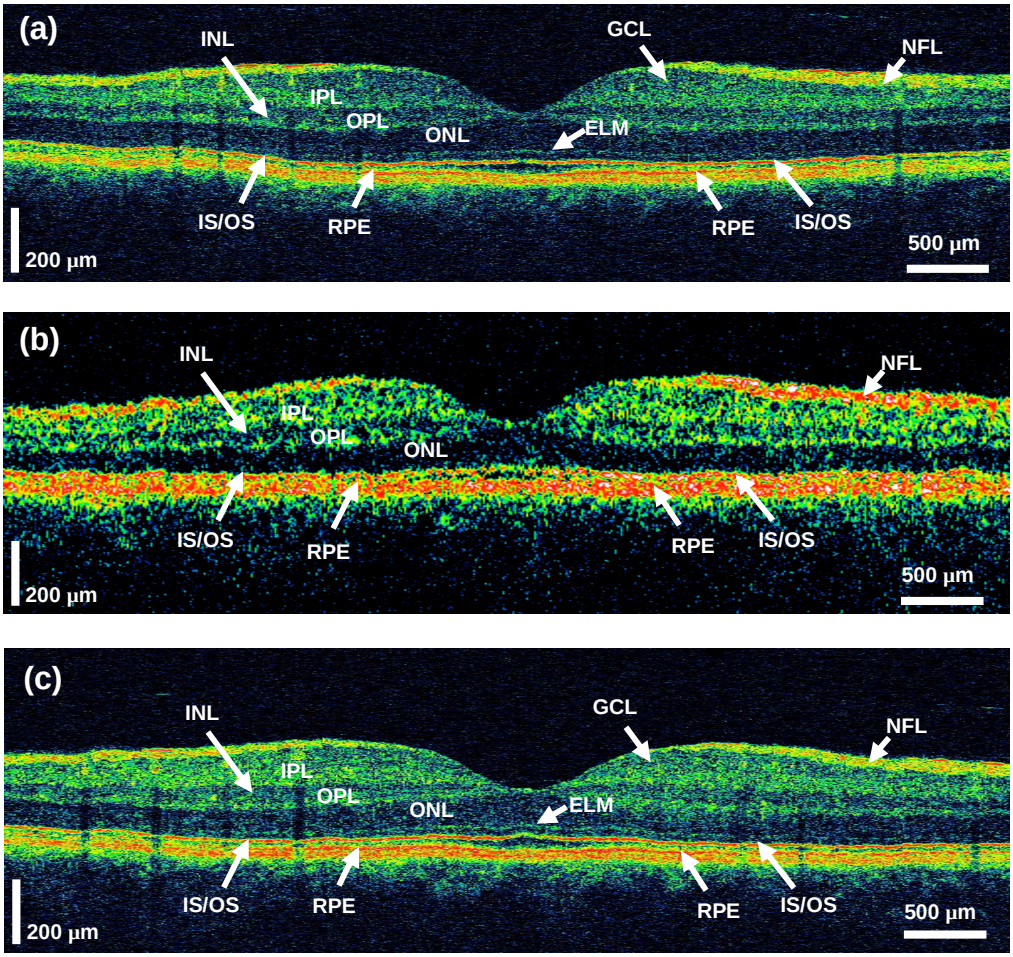

Fig. 4. OCT images of normal retina taken from the same location. a) Ultrahigh resolution OCT image taken with the Cr^{3+}:LiCAF laser with ~3.4 µm axial resolution in tissue (95dB sensitivity). b) Standard resolution OCT image taken with the commercial OCT system (Stratus OCT, Carl Zeiss Meditec, Dublin, CA) with ~10 µm axial resolution in tissue (90dB). c) Ultrahigh resolution OCT image taken with a Ti:sapphire laser with ~3 µm axial resolution in tissue (96dB). *NFL: retinal nerve fiber layer, GCL: ganglion cell layer, IPL / OPL: inner / outer plexiform layer, INL / ONL: inner / outer nuclear layer, ELM: external limiting membrane, IS/OS: junction between the inner and outer photoreceptor segment, RPE: retinal pigment epithelium.*

OCT imaging was performed with 600 µW of optical incident power in the OCT beam. This is below the 750 µW of optical incident power typically used in the commercial OCT systems, and is well within the safe retinal exposure limits at these wavelengths established by the American National Standards Institute. In order to increase the mode-locked pulse duration and reduce the peak intensities to a safe level, the output of the Cr^{3+}:LiCAF laser is sent through 100 meters of optic fiber before entering the OCT system for imaging. The interferometric point spread function of the ophthalmic imaging system, shown in Fig. 2(c), is determined by a calibrated measurement of the reflection from a mirror in the sample arm. The small asymmetry in the point spread function (PSF) of Fig. 2(c) is probably the result of wavelength dependence in the split ratio of the fiber couplers. The resolution is 4.5 µm in air,

#4498 - $15.00 US
Received 1 June 2004; revised 7 July 2004; accepted 7 July 2004

which corresponds to 3.4 μm in tissue. A sensitivity of 95 dB was obtained. The sensitivity measurement and ophthalmic OCT imaging were both performed with a detection bandwidth of 170 kHz, an axial scanning velocity of 410 mm/s, and a Doppler frequency of 1 MHz.

OCT imaging was performed in the macular region of the retina. Each OCT image consists of 3000 axial and 600 transverse pixels with an axial scan length of 1.5 mm in tissue and a transverse scan length of 6 mm. The scan repetition rate was approximately 140 scans per second and the scanning time was approximately four seconds for each image. This acquisition time is identical to that used with a femtosecond solid-state laser light source, and is sufficiently short for the subject to keep the eye open while maintaining fixation. The backscattering intensity is shown in a false-color map display to enhance visualization of intraretinal layers. Following the convention established in the commercial clinical OCT system [18,19], six radial macular scans 6 mm in length were acquired at angles separated by 30-degree intervals, thus resulting in 3 mm rays at each clock hour emanating from the fovea. Thus, OCT images obtained with different light sources can be compared with one another. In Fig. 4 (a), an ultrahigh resolution OCT image of the retina obtained with the Cr^{3+}:LiCAF source is shown. For comparison, the retina of the same healthy subject is imaged at the same location with a commercial OCT imaging system (Fig. 4 (b)) and with an ultrahigh resolution OCT system based on a mode-locked Ti:sapphire laser [20] (Fig. 4 (c)). The Ti:sapphire laser has a 125 nm bandwidth centered at 815 nm and yields ~3 μm axial resolution in tissue. By comparing the ultrahigh resolution OCT images obtained with the Cr^{3+}:LiCAF source to the standard resolution OCT images obtained from the commercial system with a SLD light source, it can be seen that the Cr^{3+}:LiCAF source produces OCT images with much better resolution because of its higher source bandwidth. Retinal structures and retinal layers boundaries are much better delineated. Specific structures, such as the ganglion cell layer and external limiting membrane, are also better visualized in the high-resolution image. In terms of image resolution and contrast, OCT images obtained with the Cr^{3+}:LiCAF source closely resemble the OCT images obtained with a Ti:sapphire laser light source. The results indicate that the ultrahigh resolution imaging performance of the Cr^{3+}:LiCAF light source approaches the performance of the Ti:sapphire laser. However, because the Cr^{3+}:LiCAF laser is directly diode-pumped, it has the advantage of being much lower cost and complexity than Ti:sapphire lasers.

4. Conclusion

We have demonstrated ultrahigh resolution OCT imaging with a diode-pumped, broadband Cr^{3+}:LiCAF laser. Retinal images with an axial image resolution of 3.4 μm in tissue were obtained with a sensitivity of 95 dB. The resolution of this light source is three times better than that of standard commercial OCT systems and is comparable to resolutions achieved with mode-locked Ti:sapphire lasers. The Cr^{3+}:LiCAF laser can be engineered into a compact and low-cost light source to perform ultrahigh resolution OCT imaging. It has the advantage that it is pumped directly by only two medium-power laser diodes. In contrast, Ti:sapphire lasers are generally pumped by diode-pumped, frequency-doubled solid-state lasers. The advantage of the diode-pumped Cr^{3+}:LiCAF laser is that it considerably reduces the complexity, cost, and power consumption. The laser can be engineered into a very compact 30 × 60 cm size including the pump lasers and further improvements in mechanical design and compactness should be possible. The Cr^{3+}:LiCAF laser provides significantly higher output powers than superluminescent diode light sources and enables higher speed and higher sensitivity imaging. Therefore, the diode-pumped Cr^{3+}:LiCAF femtosecond laser is a promising light source for a wide range of ultrahigh resolution OCT imaging applications.

This research is supported by the AFOSR Medical Free Electron Laser Program F49620-01-1-0186 and F49620-01-01-0084, NSF grants ECS-0119452 and BES-0119494, and NIH grants R01-CA75289-06 and R01-EY11289-18.

#4498 - $15.00 US Received 1 June 2004; revised 7 July 2004; accepted 7 July 2004